

Interaction between Fiber Reinforced Polymer Sheets and Concrete under Biaxial Stress Fields

by T. Furuta, T. Kanakubo, M. Uemura, and H. Yoshizawa

Synopsis:

In this research, the interaction behavior between fiber and concrete was investigated by biaxial plain loading experiments on mortar panels strengthened with various fiber sheets (carbon, aramid and glass) and analyses based on the Modified Compression-Field Theory. As result of the experiment and analysis, it was confirmed that (1) pure shear and pure tensile strengths of the strengthened panels are in proportion to the tensile strength of the fiber, (2) analysis based on the Modified Compression-Field Theory can express the experimental results excellently, and (3) in the case of fibers with small elastic modulus, there is a vast difference between local shear strains and average strains. Further analysis was conducted with the elastic modulus and weight per unit area set as the variable factors.

Keywords: biaxial properties; continuous fiber sheet; interaction; mortar panel

Tomoki Furuta is a research associate in the Department of Architecture at the Akashi National College of Technology.

Toshiyuki Kanakubo is an assistant professor in the Institute of Engineering Mechanics at the University of Tsukuba.

Masahiko Uemura is a senior fellow in the TOW SHEET division at the Nippon Steel Composite Co., Ltd.

Hiroyuki Yoshizawa is a chief engineer in the TOW SHEET division at the Nippon Steel Composite Co., Ltd.

INTRODUCTION

Currently, the strength and deformation performance of reinforced concrete members strengthened aseptically with continuous fiber sheets (hereinafter to be referred to as sheet) are, in most cases, evaluated by utilizing the existing formulas used for reinforced concrete. That of fiber in these formulas substitutes the strength of shear reinforcements. However, in actual members, it is assumed that, in addition to tensile stresses, complicated stresses are acting as well as concrete. While in the case of reinforced concrete members, the reinforcing bars yield with increasing of the deformation of member, it is possible to use the yield strength of reinforcing bars for stress evaluation. In the case of members strengthened with continuous fiber sheets this is not possible. Because the fiber stress increases as same as the increasing of fiber strain that accompanies member deformation. Therefore, for continuous fiber sheet-strengthened members, it is necessary to develop the strength evaluation method based on a detailed failure mechanism that takes into account the deformation of the members.

In order to develop the strength and deformation evaluation method based on the failure mechanism, basic data such as the interaction between the sheet and concrete are obtained and investigated in this research. This interaction involves the basic properties such as the bond, shear and tensile strengths under multi-directional stresses. To achieve these purposes, a biaxial plain loading experiment and analysis based on the Modified Compression-Field Theory are carried out.

OUTLINE OF BIAXIAL LOADING EXPERIMENT

As shown in Fig. 1 the test pieces are 300×300×15mm fiber sheet-strengthened mortar panels provided with 24 holes to fix to the loading system, and bolts to set displacement transducers. 4 types of sheets were applied on both surfaces of the mortar panel. As variable factors, the type of sheet, sheet application direction and weight per unit area were mainly selected. Loading stresses to be applied to the mortar panel were pure shear stress and pure tensile stress. Table 1 shows correspondence between each variable factor and test piece identifications. Fig. 2 shows the sheet direction of the respective test pieces. Four types of sheets were employed: commonly used $E=230\text{GPa}$ carbon fiber sheets (hereinafter to be referred to as SCF), high-elasticity ($E=500\text{GPa}$) carbon fiber sheets (hereinafter referred to as HCF), aramid fiber sheets (referred to as ARF) and glass fiber sheets (referred to as GLF). These are prepreg sheets with a weight per unit area

of 75g/m^2 . For SCF, additional test pieces of small weight (55g/m^2) and large weight (150g/m^2) sheets were fabricated. In SCF pieces for pure shear loading, sheets were applied in the directions of $45^\circ+135^\circ$, $0^\circ+90^\circ$ and $25^\circ+115^\circ$ in relation toward the side directions of the panel. For others, in the directions of $45^\circ+135^\circ$ and $0^\circ+90^\circ$. Meanwhile, for test pieces for pure tensile loading, sheets were applied in the $0^\circ+90^\circ$ direction in relation toward the direction of the panel sides. Three test pieces were fabricated for each one variable factor. Total numbers of test pieces are 48.

Premixed mortar was used with the compressive strength set to 50MPa. The mechanical characteristics of the fiber sheets and mortar are presented in Table 2 and Table 3, respectively.

For the pure shear loading, tensile forces (north-south direction) and compressive forces (east-west direction) of the same magnitudes were applied in the diagonal directions of the test pieces, using a total of 24 oil jacks (6 for each side of the panel). For pure tensile loading, tensile forces of the same magnitudes were applied by 12 oil jacks installed at the north-west and south-east positions. Displacement transducers were installed on the front surface of the test pieces in 5 directions. 3-direction strain gauges were put on the sheet surface at the center of the front and back surfaces. Fig. 3 shows the loading method, and Fig. 4 shows the positions of the displacement transducers and strain gauges.

EXPERIMENTAL RESULTS

Table 4 lists the experimental results. Photo 1 shows typical modes of failure. Fig. 5 shows the relation between shear stress and shear strain ($\tau_{xy}-\gamma_{xy}$, measured by strain gauges) for each test piece. In the test pieces subjected to pure shear loading, 2 modes of failure were observed, i.e., sheet rupture and edge failure where failure occurred at the attachment position to oil jacks. No crushing of mortar was observed. The test pieces, which failed by edge failure, were SCFH series with large-unit-weight. Though cracking observations during loading could not be carried out, the $\tau_{xy}-\gamma_{xy}$ relation for all test pieces was found to be linear up to the point where cracking is assumed to occur. In all test pieces excepting the high-elasticity HCF's, shear strain rapidly increased after the cracking. As for the HCF's, it is considered that the sheet ruptured at almost the same time with cracking. After the loading, the sheets were peeled off, and then fine hair-cracks as shown in Photo 1 (d) was observed on the putty applied on the mortar surface. The cracks, however, did not pass throughout the mortar.

Fig. 6 shows the variable factors-maximum stress relation of the test pieces. The relation between the various types of sheets with the same unit weight and maximum shear stress is shown in the Fig. 6 (a), and those for maximum tensile stress, in the Fig. 6 (b). As for SCF, the application direction of sheets of the same weight per unit area and maximum shear stress relation is presented in the Fig. 6 (c), and those for each weight per unit area and maximum shear stress, for SCF in the Fig. 6 (d). Fig. 6 (a) shows that the maximum shear stress increases, as the same as the tensile strength increases. A similar tendency is also observed in (b).

From Fig. 6 (c), no significant difference in maximum shear stress due to the application direction of the sheet was observed. As can be seen from (d), a significant tendency was observed, in which, the maximum shear stress increased as the weight per unit area also increased.

ANALYSIS BASED ON THE MODIFIED COMPRESSION-FIELD THEORY

To understanding the behavior of test pieces, analytical program based on the Modified Compression-Field Theory (1) is conducted. To adapt this method for test pieces of this research, two considerations are taken into account (2). One is the multiple-axis conversion and the other is the bond condition between fiber and mortar. The experimental results obtained by the test pieces for pure shear loading are compared with analytical results. After that, a comparative analysis is carried out for the unit weight of sheets as a variable.

The assumptive values used in the analysis are given in Table 5. As the mortar properties, values obtained by a uniaxial compression test conducted on 50-mm dia.×100mm cylinder pieces were used. For yield bond stress and slip at yield bond stress, the values obtained from Reference (3) were applied. For the sheet rupture strength, values obtained on panel test pieces subjected to pure tensile loading were used.

Table 6 compares the experimental results with the analytical results for all test pieces. The experimental results of the failure mode show full agreement with the analytical results, excepting for the test pieces that had edge failure. It is assumed that the SCFH test pieces might have crushing failure, if those had the enough capacity at the edge of attachment. The ratio of the experimental results to the analytical results on maximum shear stress ranges from 0.99 to 1.05. This means that this analysis is capable of representing the experimental results excellently.

Fig. 7 shows the analytical results of shear strain - shear stress relation for typical test pieces. The experimental results roughly agree with the analytical results. The differences between the experimental and analytical values found at the first turning point of the curves are due to the fact that the experimental values for shear strain are measured by the strain gauges, whereas, the analytical values represent mean strains. This difference was found in ARF test pieces especially. The reason for this is the fact that the difference between means strain and local one increases, as the smaller the elastic modulus of the fiber becomes.

Since the elastic modulus of fiber influences on the difference between local and mean strains, further analysis is conducted for the unit weight of sheets as a variable. Basing on the SCF's elastic modulus, unit weight of ARF and GLF is changed to have equal rigidity to SCF. As a result, unit weight of ARF and GLF is changed to 122.3 and 220.5 from 75 g/m², respectively.

The analytical results are shown in Table 7 and Fig. 8. The failure mode for both ARF and GLF in equal rigidity changes to crushing. The maximum shear stress of both exceeds that of SCF. For test pieces with fiber direction of set to 45/135°, the

Fiber Reinforced Polymer Reinforcements 675

maximum shear stress quite exceeds that of SCF. From Fig. 8, for example, if ARF's unit weight is equivalent to that of SCF, the maximum shear stress is almost the same. However, the corresponding shear strain at the same stress increases. For 45/135° test pieces, the shear stress corresponding to same strain increase in equal rigidity results. The maximum stress increases to 1.74 times of that of SCF.

It is considered that the shear strain – shear stress behavior of fiber sheets must be taken account as well as the deformation of RC members.

SUMMARY

As a result of studying the interaction between fiber and concrete, based on biaxial plain loading experiments using mortar panels strengthened with various fiber sheets (carbon, aramid and glass) as well as by analysis based on the Modified Compression-Field Theory, the following findings were obtained.

- (1) In cases of shear rupture, the pure shear and pure tensile strengths of the strengthened panel are proportional to the tensile strength of the fiber.
- (2) Analysis based on the Modified Compression-Field Theory is capable of representing the experimental results excellently.
- (3) For fibers with small elastic modulus, there is a difference between local shear strain and mean strain. Based on the results obtained by comparative analysis with the elastic modulus of sheets and the unit weight as the variable factors, elastic modulus influences the shear stress and strain relationship.

REFERENCES

- (1) Vecchio, F. J., and Collins, M. P., "The Modified Compression-Field Theory for Reinforced Concrete Elements Subjected to Shear," *ACI Structural Journal*, Vol. 83, No. 2, Mar.-Apr. 1986, pp. 219-231.
- (2) Kanakubo, T., "Analysis of Modified Compression-Field Theory for Multi-Angle Reinforcements," *Summaries of Technical Papers of Annual Meeting Architectural Institute of Japan, C-2 Structure* •, Sept. 1998, pp. 511-512. (in Japanese)
- (3) Sato, Y.; Kimura, K; and Kobatake, Y., "Bond behavior between cfrp sheet and concrete (part2) – Improvement of bond strength by out-of-plane confinement -, " *Journal of Structural and Construction Engineering (Transactions of AIJ)*, No. 509, July 1998, pp. 127-134. (in Japanese)

TABLE 1—LIST OF TEST PIECES.

Test piece	Sheet application direction	Loading method	Lot No.
SCF-0/90-CT	0° + 90°	Pure shear	6/10-2
SCF-45/135-CT	45° + 135°	Pure shear	6/23-1
SCF-25/115-CT	25° + 115°	Pure shear	6/10-1
SCF-0/90-T	0° + 90°	Pure tensile	6/10-3
SCFL-0/90-CT	0° + 90°	Pure shear	6/10-2
SCFH-0/90-CT	0° + 90°	Pure shear	6/10-2
HCF-45/135-CT	45° + 135°	Pure shear	7/13-1
HCF-0/90-CT	0° + 90°	Pure shear	7/13-1
HCF-0/90-T	0° + 90°	Pure tensile	7/13-2
ARF-45/135-CT	45° + 135°	Pure shear	6/23-1
ARF-0/90-CT	0° + 90°	Pure shear	6/23-2
ARF-0/90-T	0° + 90°	Pure tensile	7/ 1-1
GLF-45/135-CT	45° + 135°	Pure shear	6/23-3
GLF-0/90-CT	0° + 90°	Pure shear	6/23-2
GLF-0/90-T	0° + 90°	Pure tensile	7/ 1-2

SCF : Normal carbon fiber sheet (Unit weight = 75g/m²)

SCFL : Unit weight = 55 g/m²

SCFH : Unit weight = 150g/m²

HCF : High elasticity carbon fiber sheet (Unit weight = 75g/m²)

ARF : Aramid fiber sheet (Unit weight = 75g/m²)

GLF : Glass fiber sheet (Unit weight = 75g/m²)

CT : Pure shear stress

T : Pure tensile stress

45/135, 0/90, 25/115: Sheet application direction

TABLE 2—FIBER SHEET PROPERTIES.

Material	Strength (MPa)	Elastic modulus (GPa)	Unit fiber weight (g/m ²)
SCF	4,145	228.3	55
			75
			150
HCF	2,500	500.0	75
ARF	3,500	140.0	75
GLF	2,224	83.3	75

TABLE 3—MORTAR PROPERTIES.

Lot No.	Compressive strength (MPa)	Elastic modulus (GPa)	Strain at maximum stress (%)
5/28 - 1	46.6	22.2	0.364
6/10 - 1	59.7	30.1	0.296
6/10 - 2	63.4	30.2	0.294
6/10 - 3	69.0	30.7	0.316
6/23 - 1	60.5	29.4	0.278
6/23 - 2	57.9	28.2	0.272
6/23 - 3	61.3	28.6	0.286
7/01 - 1	55.5	25.2	0.329
7/01 - 2	55.6	26.5	0.319
7/13 - 1	56.9	25.6	0.321
7/13 - 2	58.2	26.6	0.297

TABLE 4—LIST OF EXPERIMENTAL RESULTS.

Test piece	Type of sheet	Loading method	Maximum shear stress (MPa)	Failure mode		
SCF-0/90-CT	Carbon (normal)	Pure shear	5.55	(Av.) 5.64	Rupture	
			5.86		Rupture	
			5.52		Rupture	
4.36			(Av.) 5.34	Rupture		
6.14				Rupture		
5.52				Edge		
SCF-45/135-CT		5.48	Pure tensile	6.11	(Av.) 5.28	Rupture
				6.11		Rupture
				4.25		Rupture
SCF-25/115-CT	4.34	Pure tensile	4.56	(Av.) 4.69	Rupture	
			4.56		Rupture	
			5.16		Rupture	
SCF-0/90-T	Carbon (light weight)	Pure shear	4.11	(Av.) 3.55	Rupture	
			2.42		Edge	
			4.14		Rupture	
SCFL-0/90-CT		Carbon (heavy weight)	Pure shear	9.36	(Av.) 7.92	Edge
				6.07		Edge
				8.34		Edge
SCFH-0/90-CT	Carbon (high-elasticity)	Pure shear	2.77	(Av.) 2.40	Rupture	
			2.45		Edge	
			2.00		Rupture	
3.15			(Av.) 2.62	Rupture		
2.71				Rupture		
2.01				Edge		
HCF-0/90-CT		1.53	Pure tensile	1.71	(Av.) 1.64	Rupture
				1.71		Rupture
				1.69		Rupture
HCF-45/135-CT	Aramid	Pure shear	5.98	(Av.) 5.74	Rupture	
			5.49		Rupture	
			5.75		Rupture	
HCF-0/90-T		5.98	Pure tensile	4.99	(Av.) 5.48	Rupture
				4.99		Rupture
				5.47		Rupture
ARF-0/90-CT	3.56	Pure tensile	3.87	(Av.) 3.78	Rupture	
			3.87		Rupture	
			3.92		Rupture	
ARF-45/135-CT	Glass	Pure shear	2.86	(Av.) 3.03	Rupture	
			3.35		Rupture	
			2.88		Rupture	
3.37			(Av.) 3.22	Rupture		
3.27				Rupture		
3.02				Rupture		
ARF-0/90-T		1.17	Pure tensile	1.12	(Av.) 1.12	Rupture
				1.12		Rupture
				1.07		Rupture
GLF-0/90-CT	1.12	Pure tensile	1.07	(Av.) 1.12	Rupture	
			1.12		Rupture	
			1.07		Rupture	
GLF-45/135-CT	1.07	Pure tensile	1.07	(Av.) 1.12	Rupture	
			1.12		Rupture	
			1.07		Rupture	
GLF-0/90-T	1.07	Pure tensile	1.07	(Av.) 1.12	Rupture	
			1.12		Rupture	
			1.07		Rupture	

TABLE 5—ANALYTICAL VALUES.

Test piece	σ_B MPa	E_c GPa	ϵ_c %	S_m mm	τ_{by} N/mm	S_{by} $\times 10^{-3}$ mm	f_{ru} MPa	E_r GPa
SCF-0/90-CT	63.4	30.2	0.294	113	4.56	1.97	1,686	228.3
SCF-45/135-CT	60.5	29.4	0.278	162	4.56	1.97	1,686	228.3
SCF-25/115-CT	59.7	30.1	0.296	162	4.56	1.97	1,686	228.3
SCFL-0/90-CT	63.4	30.2	0.294	94	4.56	1.97	1,686	228.3
SCFH-0/90-CT	63.4	30.2	0.294	162	4.56	1.97	1,686	228.3
HCF-0/90-CT	56.9	25.6	0.321	283	4.56	1.97	591	500.0
HCF-45/135-CT	56.9	25.6	0.321	70	4.56	1.97	591	500.0
ARF-0/90-CT	57.9	28.2	0.272	162	2.03	0.88	1,100	140.0
ARF-45/135-CT	60.5	29.4	0.278	226	2.03	0.88	1,100	140.0
GLF-0/90-CT	57.9	28.2	0.272	70	0.91	0.39	574	83.3
GLF-45/135-CT	61.3	28.6	0.286	94	0.91	0.39	574	83.3

σ_B : Compressive mortar strength E_c : Elastic modulus of mortar
 ϵ_c : Strain at compressive mortar strength S_m : Mean crack spacing (45°-direction)
 τ_{by} : Yield bond stress (per unit length) S_{by} : Slip at the yield bond stress
 f_{ru} : Sheet rupture strength E_r : Elastic modulus of sheet

TABLE 6—COMPARISON BETWEEN ANALYTICAL AND EXPERIMENTAL RESULTS.

Test piece	Experimental results			Analytic		Experiment / Analytic	
		Maximum shear stress (MPa)	Failure mode	Maximum shear stress (MPa)	Failure mode		
SCF-0/90-CT	-1	5.55	(Av.) 5.64	5.61	Rupture	0.99	1.00
	-2	5.86				1.04	
	-3	5.32				0.98	
SCF-45/135-CT	-1	4.36	(Av.)* 5.25	5.18	Rupture	0.84	1.01*
	-2	6.14				1.18	
	-3	5.52				Edge	
SCF-25/115-CT	-1	5.48	(Av.) 5.28	5.17	Rupture	1.05	1.02
	-2	6.11				1.18	
	-3	4.25				0.82	
SCFL-0/90-CT	-1	4.11	(Av.)* 4.13	4.11	Rupture	1.00	1.00*
	-2	2.42				Edge	
	-3	4.14				Rupture	
SCFH-0/90-CT	-1	9.36	(Av.) 7.92	8.81	crushing	—	—
	-2	6.07				Edge	
	-3	8.34				Edge	
HCF-0/90-CT	-1	2.77	(Av.)* 2.39	2.39	Rupture	1.15	1.00*
	-2	2.45				Edge	
	-3	2.00				Rupture	
HCF-45/135-CT	-1	3.15	(Av.)* 2.93	2.79	Rupture	1.12	1.05*
	-2	2.71				Edge	
	-3	2.01				Edge	
ARF-0/90-CT	-1	5.98	(Av.) 5.74	5.55	Rupture	1.08	1.03
	-2	5.49				0.99	
	-3	5.75				1.04	
ARF-45/135-CT	-1	5.98	(Av.) 5.48	5.28	Rupture	1.13	1.04
	-2	4.99				0.95	
	-3	5.47				1.04	
GLF-0/90-CT	-1	2.86	(Av.) 3.03	3.01	Rupture	0.95	1.01
	-2	3.35				1.11	
	-3	2.88				0.96	
GLF-45/135-CT	-1	3.37	(Av.) 3.22	3.24	Rupture	1.04	0.99
	-2	3.27				1.01	
	-3	3.02				0.93	

* : Except edge failure

TABLE 7—ANALYTICAL RESULTS OF UNIT WEIGHTS OF FIBER INCREASED BY ELASTIC MODULUS RATIO.

Type of fiber (Test piece)	Elastic modulus ratio	Unit weight (g/m ²)	Analytic results		$\frac{\tau_{max}}{SCF \tau_{max}}$
			Maximum shear stress (MPa)	Failure mode	
SCF-0/90-CT	—	75.0	5.61	Rupture	—
ARF-0/90-CT	1.63	75.0	5.55	Rupture	0.99
ARF equal rigidity	1.63	122.3	6.90	Crushing	1.23
GLF-0/90-CT	2.94	75.0	3.01	Rupture	0.53
GLF equal rigidity	2.94	220.5	5.63	Crushing	1.00
SCF-45/135-CT	—	75.0	5.18	Rupture	—
ARF-45/135-CT	1.63	75.0	5.28	Rupture	1.02
ARF equal rigidity	1.63	122.3	9.05	Crushing	1.74
GLF-45/135-CT	2.94	75.0	3.24	Rupture	0.63
GLF equal rigidity	2.94	220.5	7.65	Crushing	1.48

ARF equal rigidity : ARF unit weight is increased to have same rigidity of SCF.

GLF equal rigidity : GLF unit weight is increased to have same rigidity of SCF.

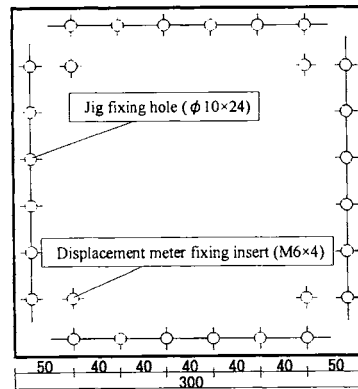


Fig. 1—Shape of test piece.

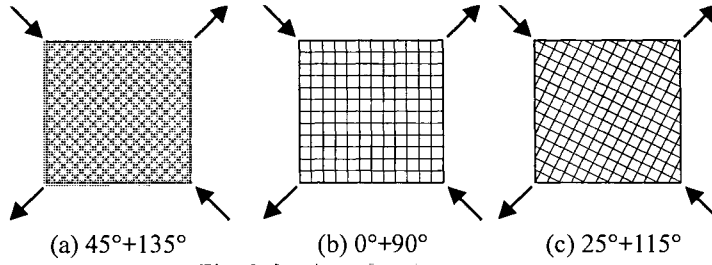


Fig. 2—Outline of each test piece.

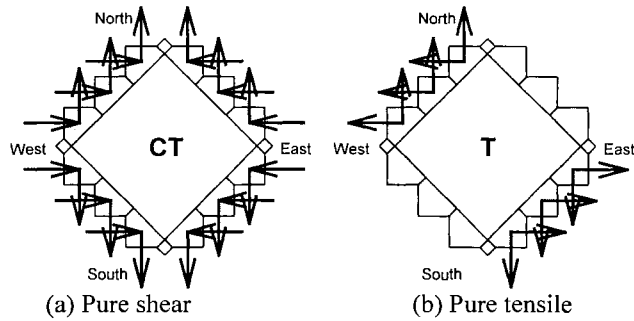


Fig. 3—Loading direction.

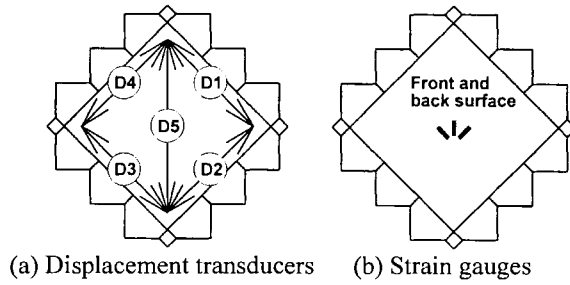
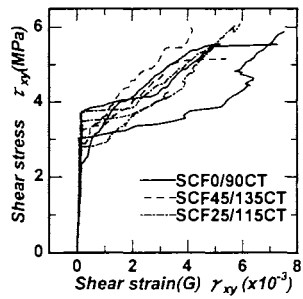
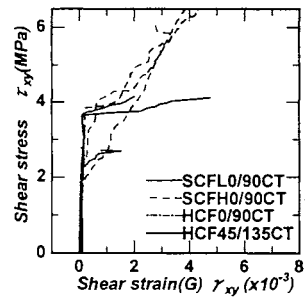


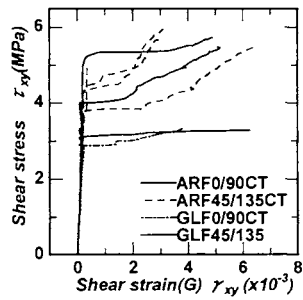
Fig. 4—Position of displacement transducers and strain gages.



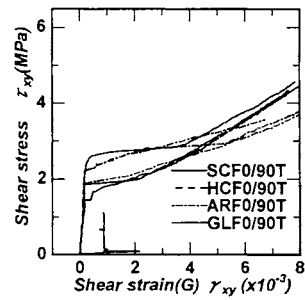
(c) ARF, GLF - Pure shear



(d) SCF, HCF, ARF, GLF - Pure tensile

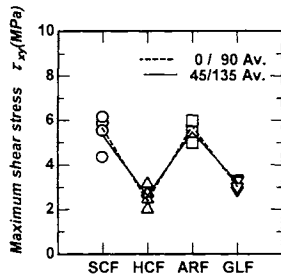


(a) SCF - Pure shear

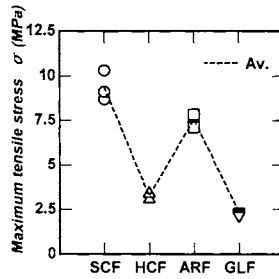


(b) SCFL, SCFH, HCF - Pure shear

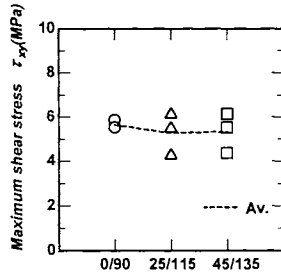
Fig. 5—Shear stress: shear strain relation.



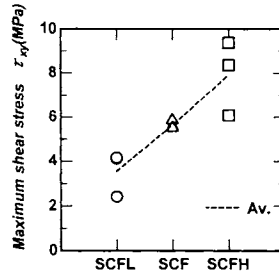
(a) Type of fiber – Maximum shear stress



(b) Type of fiber – Maximum tensile stress



(c) Fiber direction – Maximum shear stress



(d) Fiber weight – Maximum shear stress

Fig. 6—Relation between each variable factor and maximum stress.

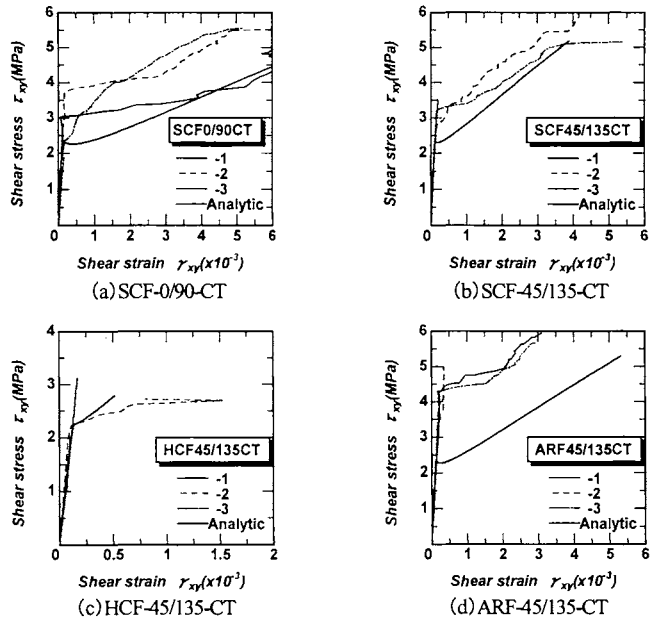


Fig. 7—Shear stress: shear strain relation.

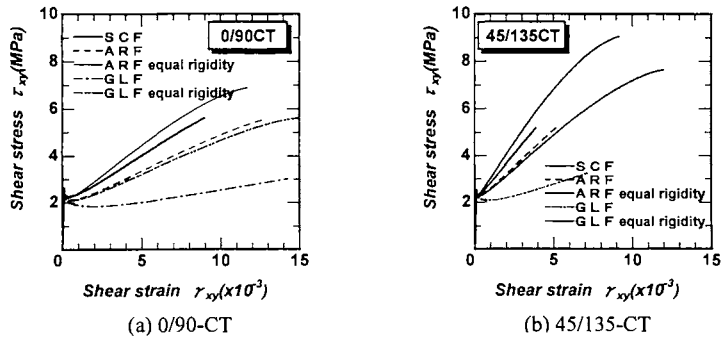
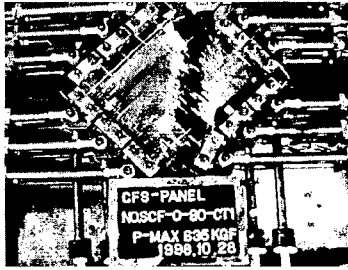
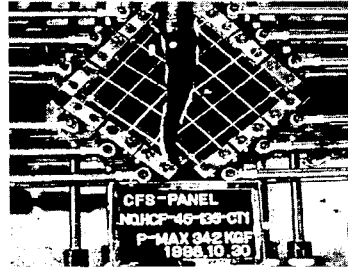


Fig. 8—Shear stress: shear strain relation (analysis).



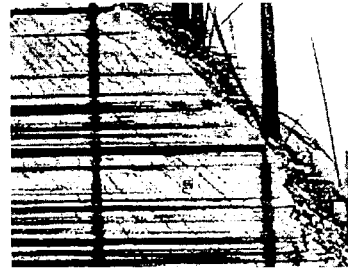
(a) SCF-0/90-CT1



(b) HCF-45/135-CT1



(c) ARF-45/135-CT3



(d) Detail of crack

Photo 1—Failure mode.